



HAL
open science

On the use of CdSe scintillating nanoplatelets as time taggers for high-energy gamma detection

R. Turtos, S. Gundacker, S. Omelkov, Benoit Mahler, A. Khan, J. Saaring, Z. Meng, A. Vasil'ev, Christophe Dujardin, M. Kirm, et al.

► **To cite this version:**

R. Turtos, S. Gundacker, S. Omelkov, Benoit Mahler, A. Khan, et al.. On the use of CdSe scintillating nanoplatelets as time taggers for high-energy gamma detection. npj 2D Materials and Applications, 2019, 3 (1), 10.1038/s41699-019-0120-8 . hal-02348053

HAL Id: hal-02348053

<https://hal.science/hal-02348053>

Submitted on 10 Dec 2020

HAL is a multi-disciplinary open access archive for the deposit and dissemination of scientific research documents, whether they are published or not. The documents may come from teaching and research institutions in France or abroad, or from public or private research centers.

L'archive ouverte pluridisciplinaire **HAL**, est destinée au dépôt et à la diffusion de documents scientifiques de niveau recherche, publiés ou non, émanant des établissements d'enseignement et de recherche français ou étrangers, des laboratoires publics ou privés.

ARTICLE OPEN

On the use of CdSe scintillating nanoplatelets as time taggers for high-energy gamma detection

R. M. Turtos^{1*}, S. Gundacker^{1,2}, S. Omelkov³, B. Mahler⁴, A. H. Khan⁵, J. Saaring³, Z. Meng⁴, A. Vasil'ev⁶, C. Dujardin⁴, M. Kirm³, I. Moreels⁵, E. Auffray¹ and P. Lecoq¹

The technological challenge imposed by the time resolution essential to achieve real-time molecular imaging calls for a new generation of ultrafast detectors. In this contribution, we demonstrate that CdSe-based semiconductor nanoplatelets can be combined with standard scintillator technology to achieve 80 ps coincidence time resolution on a hybrid functional pixel. This result contrasts with the fact that the overall detector light output is considerably affected by the loss of index-light-guiding. Here, we exploit the principle of 511 keV energy sharing between a high-Z, high stopping power bulk scintillator, and a nano-scintillator with sub-1 ns radiative recombination times, aiming at a breakthrough in the combined energy and time resolution performance. This proof-of-concept test opens the way to the design and study of larger size sensors using thin nanocomposite layers able to perform as efficient time taggers in a sampling detector geometry of new generation.

npj 2D Materials and Applications (2019)3:37

; <https://doi.org/10.1038/s41699-019-0120-8>

INTRODUCTION

The possibility of reaching real-time molecular imaging for cancer diagnosis using time-of-flight positron emission tomography scanners (TOF-PET) calls for well dedicated efforts along this line of research.¹

Benefits would extend beyond a 10-fold sensitivity, and spread to areas like neonatal imaging and theranostics, just to mention a few.² In terms of detector performance, this translates to reaching a time resolution of 10 ps, needed for 511 keV gammas to travel few millimeters within a cancer tumor. At present, the forefront time resolution values obtained in a commercially available TOF-PET scanner are at the level of 215 ps using $\text{Lu}_{2-x}\text{Y}_x\text{SiO}_5$ crystals and silicon photomultiplier (SiPM) readout.³ Time resolution achieved with current state-of-the-art scintillators featuring standard photon emission mechanisms, i.e., minimum decay times of tens of nanoseconds and maximum light yield of 100,000 ph/MeV, is largely limited by their associated photon-time density.^{4–6} Hence, harvesting prompt photons from quantum confined direct band-gap semiconductors would highly impact the time resolution of state-of-the-art scintillating detectors.⁴

Recent advances in the readout electronics of coincidence time resolution (CTR) measurements using 511 keV gammas have proven to be able to benefit from prompt emission in the form of Cherenkov photons⁷ for the purpose of improving the time resolution with standard scintillators. Unfortunately, classic Cherenkov emission in high-Z scintillators is limited up to ~20 photons emitted per 511 keV gamma interaction.^{8,9} Imposing severe limits in the number of fast photons available in the first 10 ps after the gamma has interacted. Normally, for standard state-of-the-art materials, photon-time density fluctuates ~1 photon/MeV per picosecond just from the scintillation mechanisms, not considering Cherenkov¹⁰ or hot intraband luminescence (IBL).¹¹ In order to increase the prompt photon emission yield, we

propose to replace the usual bulk scintillator pixel by a sampling configuration, so that the recoil electron from a photoelectric conversion created in the dense host scintillator can eventually reach a fast emitting nano-scintillator layer.¹² In this way, prompt or relatively prompt emission from nanocrystals could be added to the standard scintillating signal and help to decrease the overall timing jitter associated to particle detection.⁴ In this approach, each component brings its own functionality, the fast material is driving the timing improvements and the heavy/standard scintillator provides the stopping power and energy resolution.

One of the first direct band-gap semiconductor nanocrystals studied for the purpose of ultrafast timing detector applications at the level of 10 ps has been CdSe nanoplatelets.¹³ CdSe with a 1D quantum confinement and a thickness of ~1.5 nm, corresponding to 4–5 monolayers (ML)¹⁴ has been reported as one of the materials with fastest radiative recombination times due to its giant oscillator strength,^{15,16} a low stimulated emission threshold of $6 \mu\text{J}/\text{cm}^2$ and a high biexciton binding energy of ~30 meV at room temperature.^{17,18} Their red-shifted radioluminescence (RL) signal with 25% of the fast emission being unresolved by a setup with an instrumental response function (IRF) of ~130 ps full width half maximum (FWHM) and the rest being ~300 ps, makes them potential candidates for a new generation of scintillators.^{13,19} However, their implementation as radiation detectors is technologically challenging owing to intrinsic short-comings such as rather low stopping power of individual nanoparticles,^{20–23} high self-absorption owing to small Stokes-shift of emission^{24–26} and the necessary presence of organic ligands needed for surface passivation and shaping the luminescence and spatial distribution of nanoplatelets.^{27–31}

In this contribution, we focus on understanding and demonstrating the timing potential capabilities of these types of materials under ionizing radiation in section 2.1 and 2.2. The

¹CERN, Esp. de Particules 1, Meyrin 1217, Switzerland. ²Università degli Studi Milano-Bicocca, Piazza dell' Ateneo Nuovo 1, Milano 20126, Italy. ³Institute of Physics, University of Tartu, W. Ostwald Str.1, Tartu 50411, Estonia. ⁴Université de Lyon, Université Claude Bernard, Lyon 1, CNRS, Institut Lumière Matière UMR5306, F-69622 Villeurbanne, France. ⁵Department of Chemistry, Ghent University, Krijgslaan 281-S3, 9000 Ghent, Belgium. ⁶Skobeltsyn Institute of Nuclear Physics, Lomonosov Moscow State University, Leninskie Gory, 1(2), 119991 Moscow, Russia. *email: rosana.martinez.turtos@cern.ch

section 2.3 has the purpose of showing how CdSe/CdS nanoplatelets could be used in a real detector geometry for medical applications and what are the scintillating features of this type of sample. In the Discussion section, we include a study of the minimum performance needed from the CdSe-based built-up layers to reach the 10 ps goal. CdSe/CdS core-crown nanoplatelets will be studied in combination with state-of-the-art bulk materials such as LYSO, forming drop-casted films or after an embedding procedure that uses polystyrene (PS) as a host matrix. Our aim is to prove that CdSe is indeed a potential candidate for ultrafast timing applications in combination with standard scintillating technology, specially for TOF techniques using 511 keV. A second intention is to delineate a road map for the future application of CdSe nanoplatelets or similar colloidal nanocrystals with sub-1 ns decay times in a hybrid detector pixel geometry, where they are mechanically and chemically stabilized.^{4,13}

In this paper, we start from the luminescence properties of individual CdSe/CdS nanoplatelets under laser and X-ray excitation and show red-shifted biexcitonic RL at room temperature. We follow-up with a study of the light emission features of a more complex system, in which nanocrystals are either drop-casted on LYSO or forming a nanocomposite. The drop-casting technique using LYSO as direct substrate has been chosen to understand and demonstrate the timing capabilities potential of CdSe under 511 keV gamma excitation, as this method is capable of using the standard scintillator as a waveguide, transporting light to the photodetector. However, this compromises the performance of the heavy scintillator needed for the detector's energy resolution, so we follow-up with a nanocomposite approach, where CdSe/CdS nanoplatelets are mechanically stabilized on a host matrix, as this is key for real detector applications. Time-resolved ultrafast decay kinetics of a first generation CdSe-based nanocomposite under 100-fs X-ray excitation is shown together with first light output measurements obtained by X-ray attenuation and cross-checked by spectrally-resolved pulsed cathodoluminescence. We present first time results on the characterization of a sampling scintillating pixel, where standard LYSO 200 μm -thick plates are combined with CdSe/CdS nanoplatelets for 511 keV gamma detection. The promising results on the decay kinetics and time resolution obtained with a still non-optimized CdSe-LYSO sampling pixel are pushing for developing reproducible and scalable methods to produce CdSe-based built-up transparent nanocomposite layers at

least 100 μm thick in order to substitute the drop-casted films in the hybrid pixel geometry. Drop-casted films can be considered as a random distribution of "unconnected"-emitting centers, in the sense of overall energy distribution, in a given volume and they impede the application of a readout method that guarantees the ultimate performance in terms of combined energy and time resolution previously demonstrated in ref.¹²

RESULTS

Light emission properties of CdSe/CdS drop-casted films on LYSO. The core-crown heterostructure of CdSe-based nanoplatelets has been chosen owing to its enhanced quantum yield and stability compared with bare platelets.³² A first characterization of the CdSe/CdS luminescent properties under laser and X-ray excitation is performed with highly diluted films in order to avoid self-absorption. The results are shown in Fig. 1, where a clear red-shifted (lower energies) emission can be seen next to the photoluminescence (PL) line. The fit is done using a Voigt probability density function for each spectral line with similar width but centered toward lower energies. The RL data in Fig. 1b confirm the presence of a second spectral line red-shifted from 2.385 eV to 2.35 eV, i.e., equivalent to a binding energy of 35 meV, with a yield fraction of ~ 0.3 . The result of 35 meV is well in correspondence with the value reported as the binding energy of biexcitons, ~ 30 meV for bare CdSe nanoplatelets¹⁷ and it could indicate the presence of other types of multiexcitonic states. The transmission electron microscope image of the CdSe/CdS core-crown nanoplatelets used in this study is shown in Fig. 1a together with the PL emission spectra. The effective decay time under non-intense laser excitation has been measured to be ~ 600 ps, which is in very good agreement with the 520 ps found for CdSe nanoplatelets without crown.¹³ Under X-ray excitation, we obtain a faster emission towards the higher wavelengths, which reassures that the red-shifted emission is not a self-absorption artifact. The effective RL decay time is ~ 160 ps, which corresponds to both excitonic and biexcitonic spectral lines, yielding a PL/RL factor of 3.75. For further information regarding biexcitonic emission under pulsed laser excitation at different laser powers refer to Section S1.

For the purpose of detecting highly energetic particles, CdSe nanoplatelets are studied in combination with high-Z materials able to perform as state-of-the-art scintillators. The

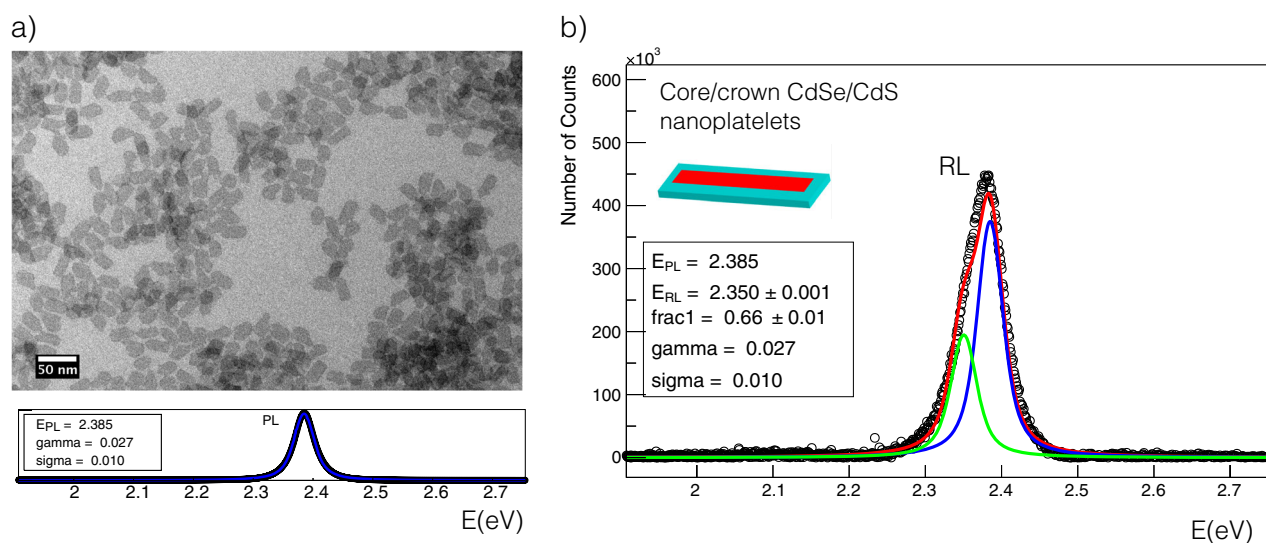


Fig. 1 Photoluminescence (PL) and radioluminescence (RL) energy spectra of core-crown CdSe/CdS nanoplatelets highly diluted films. **a** The TEM image for the CdSe/CdS synthesis is included above the PL spectra. The scale bar indicates the length of 50 nm. **b** The RL data confirm the presence of a second spectral line red-shifted from 2.385 eV to 2.35 eV, i.e., equivalent to a binding energy of 35 meV, with a yield fraction of ~ 0.3 . The Voigt function parameters characteristic of the PL spectra are shown separately in plot a)

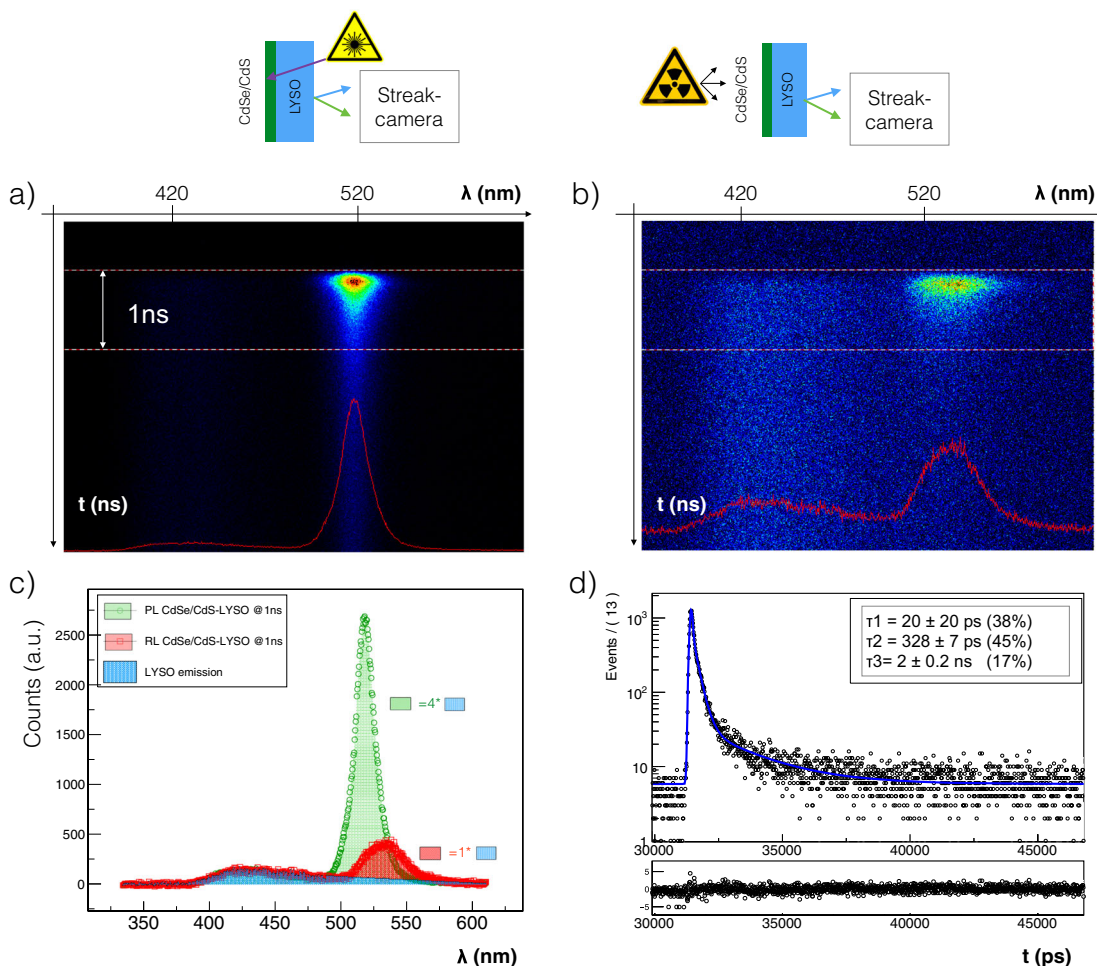


Fig. 2 Spectral-time-resolved characterization of CdSe/CdS core-crown nanoplatelets drop-casted on LYSO. Photoluminescence **a** and radioluminescence **b** time-resolved spectra of a CdSe/CdS drop-casted film deposited on a LYSO:Ce substrate as readout by a Hamamatsu streak camera. **c** Comparison of PL and RL CdSe/CdS drop-casted film spectra integrated over the first nanosecond normalized to LYSO emission. **d** Time-resolved CdSe/CdS core-crown radioluminescence integrated from 200–800 nm as measured with a hybrid PMT in time correlated single photon counting (TCSPC) mode with 130 ps FWHM instrumental response function

spectral-time-resolved PL and RL obtained for the CdSe/CdS drop-casted film on LYSO is shown in Fig. 2. The excitation and corresponding readout geometry for each measurement is shown in the schematics above the streak camera figures.

As expected, the PL emission spectra of core-crown CdSe/CdS nanoplatelets (NPLs) is centered at 515 nm and in comparison with the LYSO PL emission integrated over the first nanosecond, the signal is at least four times higher for CdSe. Taking into account the LYSO emission in the first nanosecond (1000 ph/MeV³³) and the characteristics decay times exhibited by CdSe (300 ps¹³), this measurement points towards a CdSe/CdS photon-time density at least 10 times higher than LYSO. In contrast to the PL results, under X-ray excitation we observe a large red-shift in the RL emission centered at ~530 nm, together with a decrease in the emission intensity of around a factor 75% as shown in Fig. 2c. These highlights the self-absorption issues of the drop-casted films. The comparison between PL and RL was done without moving the sample in order to keep constant the uncertainties related to focusing and alignment.

Figure 2d shows the decay kinetics of CdSe/CdS core-crown nanoplatelets under X-ray excitation. In this case, the film was drop-casted on glass to avoid the influence of LYSO emission and excited with a pulsed X-ray tube with a FWHM of ~50 ps. The photodetector used for the readout is a fast hybrid PMT and the instrumental response (IRF) function of the whole setup has been

obtained measuring the IBL of Li₂MoO₄.¹¹ The IRF has a full width half maximum of ~130 ps³⁴ and this is the reason for the unresolved first decay component expressed as 20 ± 20 ps.

CdSe-LYSO sampling pixel under 511 keV excitation

One of the benefits of improving the time resolution of scintillating detectors is applied in the TOF technique. TOF is used for particle identification in high-energy physics experiments or as a way to spatially resolve the point of positron annihilation in PET scanners. For the latest, 511 keV gammas are detected in coincidence usually by means of LYSO crystals and SiPM readout. In this section, we combine several LYSO 3 × 3 × 0.2 mm³ plates coated with the CdSe/CdS drop-casted film and we proceed with the assembly of 10 plates to form a 3.8 × 3.8 × 3 mm³ pixel shown in Fig. 3a. The aim for this kind of construction is to stop 511 keV gammas in the LYSO plates and excite the CdSe/CdS drop-casted films with the recoil electron created upon the photoelectric effect. Owing to the characteristic travel path of the recoil electron with > 400 keV, a fraction of them will be able to leak some of their energy to the nano-material and this can be observed by measuring the decay kinetics of the sampling pixel.

The time-resolved photon emission of the CdSe-based sampling pixel consisting of 10 LYSO plates 200 μm thick covered by the CdSe/CdS drop-casted films is shown in Fig. 3b. In this case, the readout takes into account all events no matter the energy

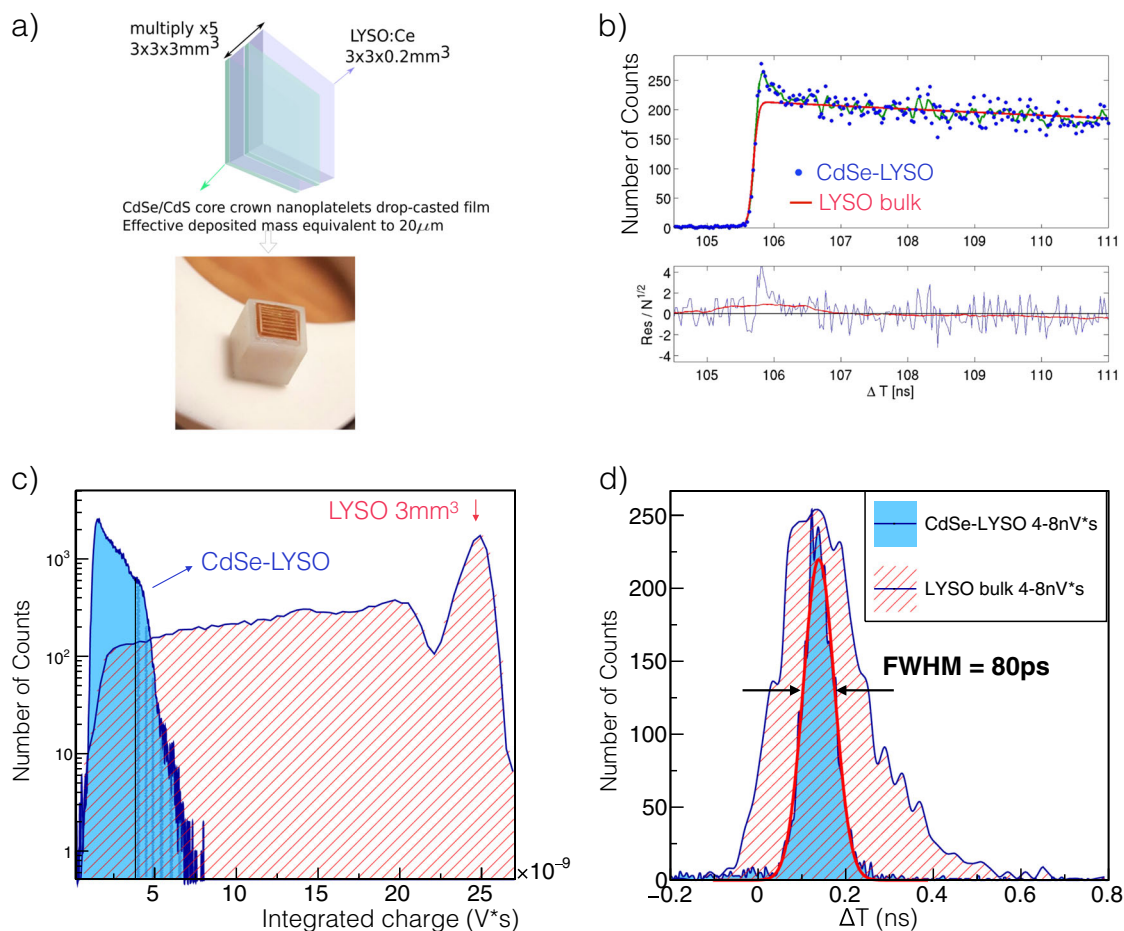


Fig. 3 Scintillation properties of the CdSe-LYSO sampling pixel measured under 511 keV gamma excitation. **a** Schematics and photo of the CdSe-LYSO sampling pixel. **b** Rise time measured in a time correlated single photon counting setup with IRF of 150 ps.⁴ **c** Energy spectrum obtained with a Na²² source, coupling the CdSe-LYSO sampling pixel to an FBK NUV-HD SiPM and triggering in coincidence with a LSO:Ce:Ca co-doped reference crystal. The same spectrum taken with a bulk 3 × 3 × 3 mm³ LYSO crystals is shown for comparison. **d** Delay time distribution for all CdSe-LYSO events in coincidence with integrated charge higher than 4 nVs. The time distribution of LYSO bulk events having a similar integrated charge between 4 and 8 nVs is shown as a reference

deposited, therefore the signal shown is characteristic for the average type of event. We observe a very fast rise time, characteristic of the first rise time component of LYSO:Ce crystals³⁵ and a prompt peak on top of the LYSO emission. The red line follows the rise time parameter of ~10 ps and the green curve represents 3–4 bins average. This measurement constitutes an experimental proof that 511 keV gamma excitation is able to transmit part of its energy to a built-up nano-scintillating layer in direct contact with the LYSO plates.

The 511 keV energy spectrum obtained by integrating the measured charge when coupling the CdSe-LYSO sampling pixel to a FBK NUV-HD SiPM³⁶ is shown in Fig. 3c. The events are in coincidence with a LSO:Ce:Ca 2 × 2 × 3 mm³ co-doped crystal used as reference with a coincidence time resolution (CTR) of 60 ps FWHM.⁷ As a form of direct comparison, the integrated charge obtained when measuring a bulk 3 × 3 × 3 mm³ LYSO:Ce crystal from the same producer than the coated plates is shown together with the CdSe-LYSO data.

As expected from the optical properties of CdSe/CdS nanoplatelets, their direct drop-casting on the surface of the LYSO disrupts the angle of total internal reflection and therefore deteriorates the index-light-guiding to the point that the photopeak and the Compton edge are not longer well separated as for the case of bulk LYSO (red stripes spectrum).

According to Fig. 3c, there is a light output reduction for the CdSe-LYSO sampling pixel of at least a factor 5, not taking into

account the SiPM saturation issues. In terms of CTR, which scales down as the square root of the photon-time density, a deterioration of a factor 5 in the number of photoelectrons detected would imply a worsening of the pixel timing performance of about a factor 2.2. Assuming plain LYSO emission, this factor translates to an expected time resolution of ~180 ps FWHM. However, looking at the delay time distribution of events in the CdSe-LYSO sampling pixel with an integrated charge higher than 4 nVs, we obtain a CTR value of 80 ps FWHM. For comparison, we have included in Fig. 3d the delay time distribution obtained with bulk LYSO crystal, choosing events with a similar integrated charge from 4 to 8 nVs.

Despite all the optical issues, drop-casted films allow to mechanically assemble a CdSe-LYSO sampling pixel for a first time proof-of-concept with 511 keV gammas. An extended study of a second type of sampling pixel using Bi₄Ge₃O₁₂ as high-Z material is included in the Supplementary Information Section S2, Fig. S2. The CTR of this crystal is determined by its Cherenkov emission at a level of few photons, instead of by its standard photostatistic and this has a crucial role in the readout threshold and depth of interaction correction needed in long sensors. Therefore, the study of this type of combination, Cherenkov emitter and fast nanocrystals is complementary to the LYSO case.

The results presented above constitute an experimental proof that CdSe nanoplatelets bears significant timing potential for 511 keV gamma detection. However, its assembly in combination

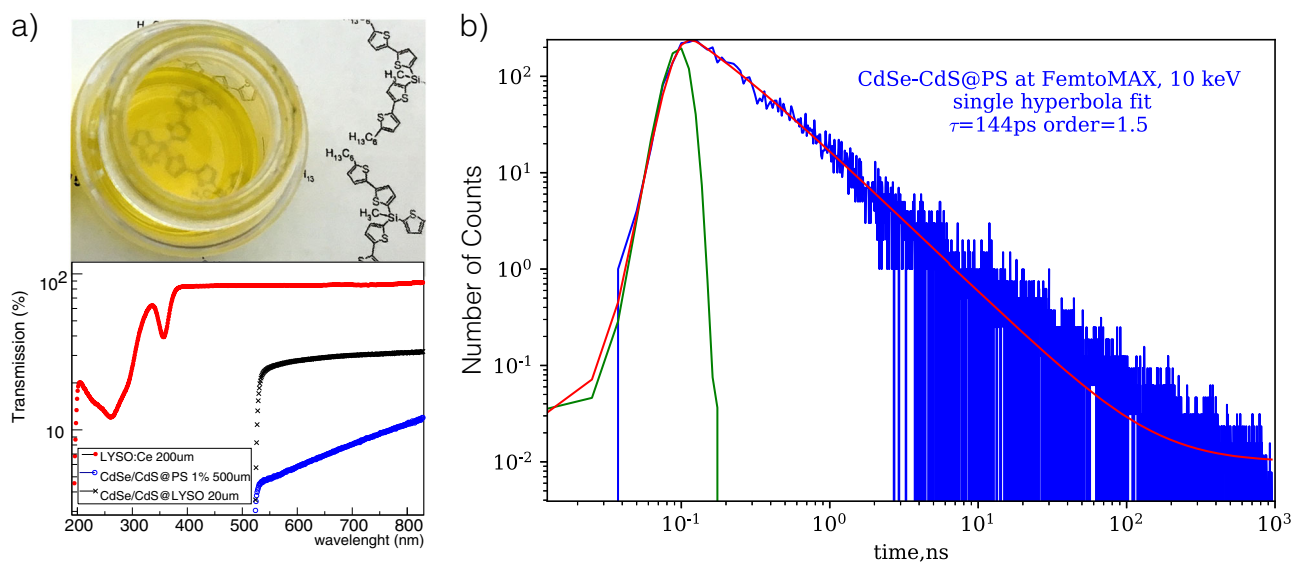


Fig. 4 Scintillating kinetics of CdSe-based nanocomposite 1% weight concentration. **a** Transmission of CdSe/CdS nanocomposite 1% weight concentration 500 μm thick and CdSe/CdS drop-casted film with an effective thickness of 20 μm in comparison with LYSO:Ce crystal 200 μm thick. **b** Time-resolved decay kinetics of CdSe/CdS@PS 1% as measured at the FemtoMAX beamline with a IRF of 38 ps FWHM. The double-logarithmic scale has been chosen for better visualization of the data

with state-of-the-art scintillators must be optimized. This work proves that CdSe nanoplatelets, if properly stabilized as emitting centers in a matrix host, would revolutionize the field of fast timing research and the new detectors could eventually reach the regime of real-time molecular imaging in the clinical scenario. Our efforts in this direction are described in the section below.

Light emission properties of CdSe-based nanocomposite under X-ray and electron excitation

The decay kinetics of CdSe/CdS nanocomposite in a polystyrene (PS) host (CdSe/CdS@PS) with 1% weight concentration has been obtained with exceptional time resolution of 38 ps FWHM at the FemtoMAX beamline in Lund, Sweden. Time-resolved data are shown in Fig. 4 together with the setup IRF. We observe a fast photo-response, which decays two order of magnitudes in the first 10 ns according to Fig. 4b, (for further fitting details with multi-exponential decay components refer to Table S1). These results are found to be in good agreement with the PL study performed with similar nanoplatelets using long integration gates up to 20 μs .³² In addition to the rise-decay kinetics, Fig. 4a shows the prepared sample and its transmission in comparison with CdSe/CdS drop-casted films and LYSO plates up to 200 μm thick.

Concerning light output under high excitation, the two-step light yield characterization results obtained for the CdSe-based nanocomposite sample are shown in Fig. 5. Both samples, LYSO and CdSe/CdS@PS 1% have the same cross section size of $3 \times 3 \text{ mm}^2$ and were excited by a collimated X-ray beam of 3 mm diameter. The CdSe/CdS@PS 1% light output is obtained by comparing to the amount of photons integrated over a pre-defined 500 ns gate using the LYSO as reference. Taking into account LYSO intrinsic yield³³ and its reported non-proportionality of $\sim 55\%$ for 10 keV gammas, we obtain a reference value of 22,000 ph/MeV. A direct comparison of the decay curves obtained for both samples, LYSO (reference) and CdSe/CdS@PS 1% is shown in Fig. 5a for the first 10 ns of scintillating signal next to the sample X-ray attenuation. For further details regarding the light yield determination measurements consult the Methods section and for a full review using different materials refer to ref.³⁴

A summary of the measured absorption coefficient and comparative light yield value obtained for the CdSe-based nanocomposite sample is shown in Table 1. Summing up the

two-step light yield measurements result in a value no higher than 100 ph/MeV.

A second method to determine the light yield of the nanocomposite sample uses short range electron excitation. The procedure of pulsed cathodoluminescence yield comparison of transparent samples (crystals or PS slabs) was described in.³⁷ Similarly to the drop-casted CdSe/CdS nanoplatelets under continuous electron beam,³⁴ the same nanoplatelets embedded in polystyrene (PS) have shown some degree of CL degradation under 120 keV electron pulses. The peak pulse electron current was reduced to 0.7 A/cm² to partially mitigate this effect. Owing to the pulsed nature of the source, the first spectrum was recorded with no preliminary irradiation and can be considered unaffected by degradation as shown in Fig. 6, curve 1. The repeated measurement indicated $\sim 20\%$ loss of yield after full spectral scan (which takes $\sim 300\text{--}400$ electron pulses).

Figure 6 shows the spectra of CdSe/CdS@PS and LYSO:Ce, recorded in 0–200 μs time window in the same conditions. Such time window was selected to ensure that all the luminescence has completely decayed during acquisition, so that the total yield of different emissions can be compared. The spectrum consists of three separate emission bands: PS host luminescence at 330 nm, CdSe/CdS excitonic band at 525 nm and broad defect emission at ~ 750 nm. The absence of the latter in the spectrum recorded in 0–32 ns time window indicates that it has the decay constant in microsecond range, which could not be measured in our experiment. The decay curves of 330 nm and 525 nm bands are complex and the list of their exponential decay components is shown in Table S1. Both high-energy X-rays and electron beam pulses populate high excited states, wherefrom energy is transferred to the emission centers through various relaxation processes causing appearance of complicated decay curves. It should be noted that the main component of PS emission (15 ns) is very similar to the slow component of excitonic emission (18 ns), which indicates that about half of the total excitonic yield in cathodoluminescence experiment comes from re-absorption of slow PS emission. Comparing decay kinetics between the different experiments shows that the decay component of 300 ps is only preserved for the X-ray experiment at CERN where the beam flux does not degrade the luminescence properties of CdSe/CdS@PS 1% sample. For an extended study of this method with a different

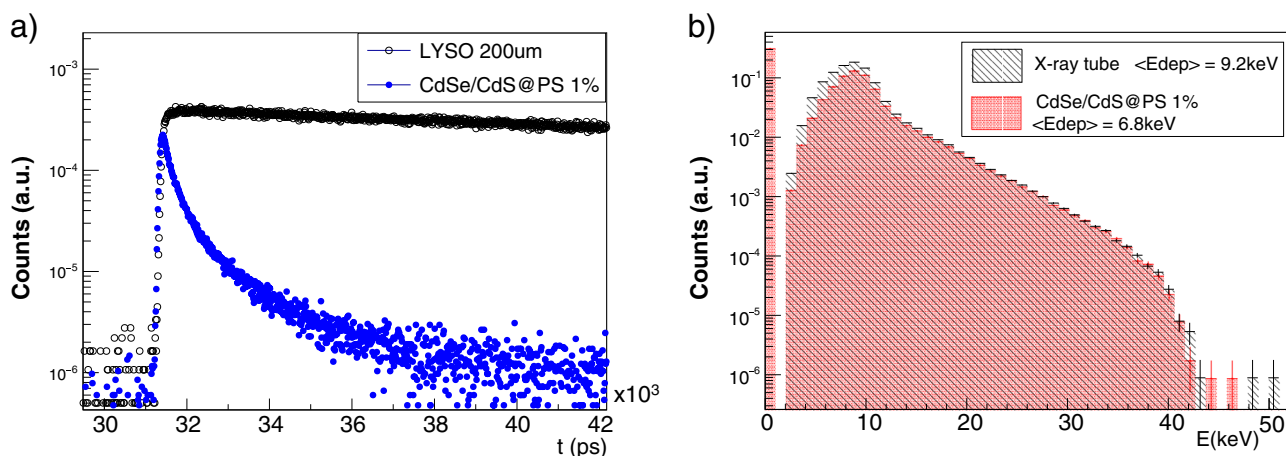


Fig. 5 Two-step light yield determination of CdSe/CdS@PS 1% sample. **a** Comparative light output between LYSO and CdSe/CdS@PS 1% obtained in a time correlated single photon counting setup with a tungsten pulsed X-ray tube up to 40 kV. Data are shown within a 10 ns gate for visual purposes. **b** X-ray attenuation measured with the Timepix chip detector⁴⁵

Table 1. Measured absorption coefficient η , comparative light output and light yield for a CdSe/CdS@PS 1% nanocomposite sample measured under soft X-ray excitation up to 40 keV

Nano-scint	LY_{est}^1 %	η_{TPX}	LY_{meas} (ph/MeV)	$Yield_{1ns}^2$ %	$Yield_{10ns}^2$ %
CdSe/CdS@PS 1%	0.1	0.26	85	60	83

¹Estimated light yield as compared with the LYSO intrinsic light yield at 10 keV and assuming full energy deposition

²The Yield1ns and Yield10ns represent the percentage of the emission integrated over 1 ns or 10 ns with respect to the total emission integrated over 500 ns

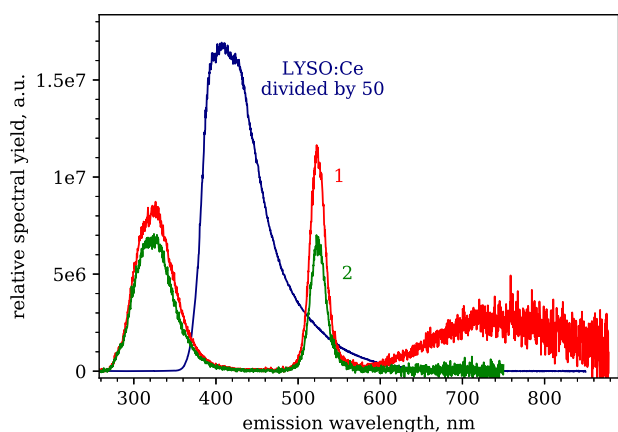


Fig. 6 High-energy cathodoluminescence emission spectra of CdSe/CdS@PS 1%. Curve (1) was recorded in the 0–200 μ s time gate and curve (2) between 0 and 32 ns time window relative to the excitation pulse. The CL spectrum of LYSO:Ce was recorded in 0–200 μ s time window

type of nanocrystals refer to the Supplementary information Section S4.

The approximate light yield numbers can be derived from the first spectra for which the degradation of the sample was negligible (Fig. 6, curve 1). The total light yield of 525 nm excitonic band in 0–200 μ s time window is 0.37% of total LYSO:Ce cathodoluminescence yield. The non-proportionality of LYSO:Ce

at 100–120 keV X-ray is 80–85% relative to the yield at 662 keV.³⁸ Assuming the same non-proportionality factor for the electron beam, the excitonic emission yield (525 nm line) is 122 ph/MeV, of which only 68 ph/MeV belong to the ultrafast components with decay constant $\tau \leq 1.1$ ns. For comparison, the yield of PS emission band and defect band is 0.63% and 0.62% of LYSO:Ce, respectively, and, combined together, comprise 77% of total light output of CdSe/CdS@PS.

In this experiment, we can assume that most of the energy is absorbed by PS because the electron penetration depth is no more than 0.2 mm and most of the material encountered by electrons on that distance is PS. Therefore, the ratio of excitonic to PS emission in this case will correspond to the energy transfer efficiency from PS to NPLs. The ratio of surfaces under 520 nm and 320 nm bands in Fig. 6, curve 1 is 0.58. However, not all of the 520 nm emission is caused by prompt processes, and to estimate the efficiency of prompt energy transfer we have to subtract the effect of delayed energy transfer. The total yield of PS and excitonic bands is 0.63 and 0.37% of LYSO standard, respectively. In all, 55% of excitonic emission is prompt ($\tau \leq 1.1$ ns), and the rest is somehow delayed. Owing to the similarity of decay components of delayed NPLs emission and PS emission (as described above) we can assume the main reason of delayed energy transfer is re-absorption. Taking the quantum efficiency of NPLs as $\sim 50\%$,³² we can estimate which portion of PS emission was reabsorbed by NPLs. After correcting for re-absorption in this way, the ratio of intrinsic PS yield to prompt excitonic yield becomes 0.21. This value is in a very good correspondence with 20–25% obtained by theoretical considerations (Supplementary information Section S3.).

DISCUSSION

As presented in the sections above, CdSe/CdS nanoplatelets exhibit a red-shifted RL emission with a binding energy of 35 meV, characteristic of biexcitons in 1.5 nm thick CdSe platelets. This confirms biexcitonic emission under X-ray excitation, which have associated decay times of ~ 100 ps, a promising route to pursue for fast timing applications.

As expected, CdSe/CdS drop-casted films using LYSO as substrate affect the light transport within LYSO itself, given by the angle of total internal reflection. Optically separating the standard and the fast photon emission phases would allow for a better performance of the sampling pixel. In this regard, we studied the luminescence properties of CdSe/CdS nanoplatelets embedded in PS as a way to build a nanocomposite suitable for

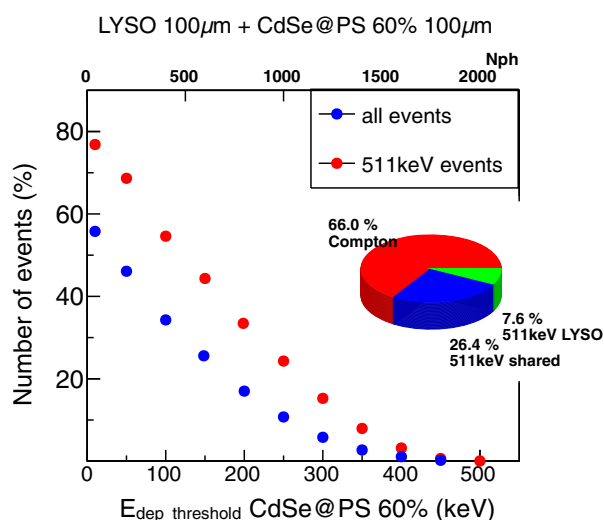


Fig. 7 In total, 511 keV gamma energy distribution in a sampling pixel geometry able to provide ultimate timing. Geant4-based simulations were done for a hybrid pixel consisting of 100 μm thick LYSO plates combined with 100 μm thick layers of CdSe-based nanocomposite with a loading fraction of 60% in polystyrene. The blue (red) solid dots show the % of events with respect to the total number of detected events (511 keV events) for which the energy deposited in the nano-phase surpasses the energy value indicated in the x axis. The number of photons given per energy deposited in the upper X axis corresponds to the minimum estimated value able to provide ultimate time resolution at energies above 250 keV (see Fig. S6)

the detection of high energetic particles in combination with high-Z materials. The light output of this nanocomposite with 1% weight concentration have been characterized using X-ray and electron excitation, yielding very modest values of ~ 100 ph/MeV. Calculations of the range for non-radiative energy transfer between the organic host and the inorganic nanoparticles are able to estimate an effective volume surrounding the nanoplatelets for which the transfer is highly probable (see Fig. S4). For the given weight concentration of 1%, effective non-radiative energy transfer accounts at most for just 20% of the energy deposited in the PS host. Weight concentrations of at least 10%, where the average distance between nanoplatelets would be on the order of 30 nm would significantly increase the amount of energy transfer by dipole-dipole interactions, i.e., up to 20% without considering exciton diffusion (see Section S3 of Supplementary information).

A sampling pixel geometry with optically separated scintillators has been previously implemented and proven to bring better timing to a fraction of the 511 keV events.¹² The experimental proof-of-concept readout has been implemented with BC-422, a plastic scintillator in the shape of 200 μm thin plates combined with 200 μm thin plates of LYSO or BGO. This plastic scintillator presents a very low density of 1.0 g/cm³ (no-photopeak), a minimum decay time of 1.3 ns, light yield of 10,000 ph/MeV and therefore an excellent CTR of 35 ps FWHM. Therefore, substituting the BC-422 material by CdSe-based nanocomposites layers up to 100 μm thick with weight concentrations of minimum 10% and ultimate timing constitutes a solution for the material bottlenecks faced in fast timing applications.

In this regard, the last developments in the production of high-loaded nanocomposites with weight concentrations up to 60% are showing excellent transmission values at the level of 60–80% for 2 mm-thick samples as reported in.³¹ In this study, they report on a chemical path that allows for ligand-functionalized CdZnS/CdS quantum dots to be covalently bound to the polymer host, resulting in nanocomposites samples with high light yield and enhanced probability of gamma conversion.

The inclusion of a dye molecule acting as a wavelength shifter enlarges the small Stoke-shift characteristic of direct band-gap semiconductors and modulates the sample's transparency to values up to 80%. In the case of CdSe nanoplatelets, particles synthesized with 5 monolayers (ML) instead of 4 ML (the ones presented in this study) have been proven to emit at 550 nm and to present ultrafast interplate Förster energy transfer when used in combination with the 4 ML nanoplatelets.³⁹ This ultrafast energy transfer mechanism with lifetimes of ~ 28 ps between emitting centers with a spectral overlap could be used as a non-radiative wavelength shifting process able to preserve fast rise-times critical for timing applications.

Aiming at the optimization of such hybrid pixel, Geant4 simulations^{40,41} of the energy deposited by 511 keV gamma rays are used for the estimation of the fraction of energy going to each scintillator on an event-by-event basis. This distribution is shown in Fig. 7 for a hybrid pixel composed of LYSO plates 100 μm thick and CdSe-based nanocomposite with a loading fraction of 60%, also 100 μm thick. The total number of events detected are $\sim 20\%$ of the total, which compares to 22% for the case of bulk LYSO $3 \times 3 \times 3$ mm³. Regarding the distribution of events fully depositing 511 keV within the sampling pixel they account for 34% of the gammas detected. We observe that a minority of such events, 8% are not able to share energy and therefore will carry standard timing resolution. However, the majority of 511 keV events, more than two-thirds, would enter in the category of shared events, having energy deposited in both scintillators. For this configuration, they will represent 26% of the events and they will exhibit improved time resolution.

These calculations show the incredible application potential of having a highly loaded mono-disperse nanocomposite up to 100 μm thick in combination with LYSO or other high-Z scintillators with similar density. Not only the total number of detected events is 90% compared with bulk LYSO, but the number of events depositing >200 keV in CdSe-based nanocomposite represents $\sim 30\%$ of the events depositing 511 keV in the sampling pixel. The transmission/transparency of a mono-disperse highly loaded nanocomposite with thickness of 100 μm is a topic for further investigation, as well as the chemical path leading to such high loadings for this type of nanoplatelets.³¹

This paper reports on the very encouraging results from a proof-of-concept experiment exploring the use of CdSe-based nanoplatelets in combination with standard detector technology in a hybrid functional pixel. Integrating fast emitting nanocrystal semiconductors with state-of-the-art scintillators is shown here as a pathway for improved timing performance, which otherwise faces severe limitations.

We are able to observe for the first time CdSe/CdS scintillation emission under 511 keV gamma excitation in the form of a prompt peak added to the LYSO characteristic kinetics. This prompt emission has proven to reduce the timing jitter associated with 511 keV gamma detection, yielding CTR state-of-the-art values of ~ 80 ps.

In view of the upgraded detector pixel geometry, we foresee the need for a CdSe-based built-up nano-scintillating layer with a minimum thickness of 100 μm . Aiming at higher nanocomposite loadings of at least 10% weight concentration is essential in order to harvest most of the energy deposited in the polymer matrix. On top, increasing the total light yield of CdSe-based nanocomposite in a factor 100, would provide with the photon-time density critical to reach ultimate time resolution for a significant fraction of the events fully contained in the proposed hybrid pixel geometry.

This proof-of concept test opens the way to the design and study of larger size sensors aiming at a high sensitivity and picosecond timing resolution in the low energy detection regime of few hundreds keV.

METHODS

Luminescence properties of CdSe/CdS core-crown nanoplatelets

CdSe-based samples consist of CdSe 4 ML in the form of nanoplatelets synthesized by wet chemical methods (protocol established in¹⁵). After the main synthesis, a second one follows in order to add a CdS crown around the CdSe nanoplatelets as reported in ref.⁴²

The spectroscopy of drop-casted CdSe/CdS films using LYSO as substrate was measured with a Hamamatsu streak camera model C10910. The PL was obtained using a PILAS picosecond pulsed diode laser with wavelength of 372 nm as source of excitation with ~45 ps FWHM. Meanwhile, the RL data use a Hamamatsu 50 ps FWHM pulsed X-ray tungsten tube with energies up to 40 keV and lines centered between 9 and 11 keV. For these measurements, we have used LYSO:Ce from Crystal Photonics Inc., $3 \times 3 \times 0.2 \text{ mm}^3$ as a substrate for the film preparation and the nanoplatelet deposition covers one of the two $3 \times 3 \text{ mm}^2$ polished faces. The emission is collected in transmission mode through the 200 μm thick LYSO crystal and integrated over the first 5 ns. The effective thickness of the film deposited on LYSO used for the PL and RL measurements is estimated to be ~20 μm given by the amount of CdSe deposited and assuming all the nanoplatelets are forming a bulk layer.

CdSe-LYSO sampling pixel under 511 keV gamma excitation

For the rise-decay time measurement under 511 keV excitation, we use a time correlated single photon counting (TCSPC) setup with an IRF of 150 ps FWHM measured with Cherenkov emission in undoped LuAG crystals. The start detector consist of a LSO:Ce:Ca co-doped crystal coupled to a SiPM and an ID Quantique performs as stop detector. For more details regarding the specifications and previous data taken with this setup please refer to ref.³⁵

The CTR measurements were performed in the state-of-the-art experimental setup previously described in^{7,12}. This bench uses a LSO:Ce:Ca $2 \times 2 \times 3 \text{ mm}^3$ crystal as reference detector with a single time resolution of 41 ps FWHM. The SiPMs in used are FBK NUV-HD with 40 μm SPADs size³⁶ and measured single photon-time resolution of 70 ps. The electronics readout divides the integrated signal to perform separate measurements of energy and timing and a high-frequency amplifier⁴³ with 1.5 GHz bandwidth is used to record the time stamps. The signals are analyzed in a Lecroy oscilloscope with 3.5 GHz bandwidth and 40 Gs/s (using four channels this reduces to 20 Gs/s, i.e., 50 ps binning). The sampling pixels are coupled to the SiPMs using Meltmount glue with an index of refraction of 1.582, which allows for a good index matching with the photodetector.

CdSe/CdS embedded in polystyrene at 1% weight concentration

The CdSe-based nanocomposite followed an embedding procedure where the colloidal nanoplatelet solution is mixed with dissolved pure PS, evaporated and dried. The CdSe/CdS core-crown solution has been synthesized with a cadmium concentration of ~4.4 g/L (0.3 absorbance at 350 nm), from which 1 mL is mixed in 300 mg of PS. The weight concentration for this sample is ~1% and the overall thickness of the CdSe/CdS nanocomposite is ~0.5 mm.

The decay kinetics of CdSe/CdS@PS 1% weight concentration nanocomposite with an exceptional time resolution of 38 ps FWHM was studied during feasibility test beamtime at FemtoMAX⁴⁴ short-pulse facility (SPF at MAX-IV laboratory, Lund, Sweden). The beamline provided 10 keV monochromatic X-ray pulses of 100 fs width (FWHM) at 2 Hz. The scintillation photons were detected by Hamamatsu R3809U-50 MCP-PMT through SCHOTT GG475 long-pass filter. The MCP-PMT operated in a single photon counting mode with a transit time spread of 25 ps FWHM (according to the datasheet). The output of the detector was boosted by an SHF 100 APP broadband preamplifier (12 GHz, 19 dB) and digitized by the Lecroy Labmaster 10–36Zi oscilloscope (36 GHz, 80 G s/s). The trigger for the oscilloscope was a signal induced in the RF antenna by electron beam passing the SPF undulator.

After each excitation pulse a waveform containing several single photon peaks correlated with the trigger event was obtained. Each waveform was processed in LabView by its built-in Peak Detector Virtual Instrument, which detected photon time stamps. The decay curves were obtained by accumulating those time stamps over 6–12 hour period, and plotting them on a histogram with 12.5 ps bin width (equal to oscilloscope sampling period). For the determination of IRF of a system we recorded the decay of IBL in Li_2MoO_4 crystal using SCHOTT GG420 long-pass filter, and applied Gaussian fit to the recorded curve. The IBL is a prompt weak emission³⁷ with decay times on the order of 1 ps, and, in all experiments known to us, its time

profile repeated the IRF of the system. The luminescence of air having decay time of ~0.5 ns was suppressed by the long-pass filters used, as it was shown to have negligible intensity at wavelengths longer than 420 nm.

Light yield measurements under X-ray excitation

The light output study is done by comparing the emission from nanocomposites to the light collected from a LYSO crystal in the same excitation conditions, normalizing to its intrinsic light yield and assuming full energy deposition. All samples are placed in the same position, irradiated with a X-ray beam collimated to 3 mm diameter and readout using the same integration time window of 500 ns. Measurements were performed in time correlated single photon counting mode using a fast hybrid PMT (HPM-100-07 from Becker&Hickl) connected through a constant fraction discriminator (ORTEC 9327) to a fast TDC (the xTDC4-PCle from Cronologic). The IRF of the setup has been obtained by recording the time response of IBL present in Li_2MoO_4 crystals, which has shown FWHM of ~130 ps. For more details, please consider³⁴

X-ray absorption by nano-scintillating layers is used to evaluate the energy deposited by X-rays in the samples under study. For this, we use the Timepix chip from the Medipix collaboration at CERN as X-ray detector.⁴⁵ We monitored the attenuation of the X-ray beam as it passes through the samples and report an attenuation coefficient η , which it is to correct by the partial energy deposition.

As the X-ray tube energy spectra is not mono-energetic, we use the mean value of the energy deposited in the X-ray detector as a way to compute the energy deposited on the nanocomposite sample. In this regard, we find the mean energy deposited in the sample of interest by subtracting the detector response with and without sample in between the X-ray beam and the detector as it follows:

$$\eta = \frac{\langle E_{dep}^{NCs} \rangle}{\langle E_{dep}^{TPX} \rangle} = \frac{\langle E_{dep}^{TPX} \rangle - \langle E_{dep}^{TPX} \rangle^{NCs}}{\langle E_{dep}^{TPX} \rangle} \quad (1)$$

Here $\langle E_{dep}^{TPX} \rangle^{NCs}$ is the mean energy deposited in the Timepix detector when the nanocomposite is in place.

Light yield measurements under electron excitation

We use a spectral-time-resolved cathodoluminescence setup with a broad energy electron beam and $E_e^{max} = 120 \text{ keV}$ (with penetration depth of ~0.2 mm) to probe the energy transfer mechanisms within CdSe-based nanocomposites.

The spectra and decays were obtained at the pulsed cathodoluminescence setup described in ref.¹¹ The electron beam with 200 ps FWHM pulse and peak electron current of 10 A/cm^2 was used as source of excitation. The Andor iStar iCCD was used to obtain the gated spectra in different time windows. For decay curves, a Hamamatsu R3809U-50 MCP-PMT was used, with a time response of 250 ps FWHM. A total time window for luminescence monitoring after the excitation pulse was 50 μs . The IRF was determined by measuring the time profile of hot IBL of PbF_2 single crystal. The samples of CdSe/CdS@PS and LYSO:Ce were installed on the sample holder, and covered by identical aluminum masks to expose the same sample surface area (~4 \times 8 mm^2) to the wide homogeneous electron beam. The samples could be positioned in front of the beam by the means of the manipulator, which enables precise comparison of the sample light output in the same conditions.

DATA AVAILABILITY

The data sets generated during and/or analyzed during the current study are available from the corresponding author on reasonable request.

Received: 17 April 2019; Accepted: 10 September 2019;

Published online: 04 October 2019

REFERENCES

1. The 10 ps challenge, a step toward reconstruction-less TOF-PET. [Online]. Available: <https://the10ps-challenge.org>.
2. Lecoq, P. Pushing the limits in Time-of-Flight PET imaging. *IEEE Trans. Radiat. Plasma Med. Sci.* **1**, 473–485 (2017).
3. Biograph vision. [Online]. Available: <https://www.siemens-healthineers.com/molecular-imaging/pet-ct/biograph-vision>.

4. Gundacker, S., Auffray, E., Pauwels, K. & Lecoq, P. Measurement of intrinsic rise times for various L(Y)SO and LuAG scintillators with a general study of prompt photons to achieve 10 ps in TOF-PET. *Phys. Med. Biol.* **61**, 2802 (2016).
5. Nikl, M. & Yoshikawa, A. Recent R&D trends in inorganic single-crystal scintillator materials for radiation detection. *Adv. Opt. Mater.* **3**, 463–481 (2015).
6. Dujardin, C. et al. Needs, trends, and advances in inorganic scintillators. *IEEE Trans. Nucl. Sci.* **65**, 1977–1997 (2018).
7. Gundacker, S., Turtos, R. M., Auffray, E., Paganoni, M. & Lecoq, P. High-frequency SiPM readout advances measured coincidence time resolution limits in TOF-PET. *Phys. Med. Biol.* **64**, 055012 (2019).
8. Korpar, S., Dolenc, R., Križan, P., Pestotnik, R. & Stanovnik, A. Study of TOF-PET using cherenkov light. *Nucl. Instrum. Methods Phys. Sect. A, Accel. Spectrom. Detect. Assoc. Equip.* **654**, 532–538 (2011).
9. Brunner, S. E., Gruber, L., Marton, J., Suzuki, K. & Hirtl, A. Studies on the Cherenkov effect for improved time resolution of TOF-PET. *IEEE Trans. Nucl. Sci.* **61**, 443–447 (2014).
10. Brunner, S. E. & Schaart, D. R. BGO as a hybrid scintillator/cherenkov radiator for cost-effective time-of-flight PET. *Phys. Med. Biol.* **62**, 4421–4439 (2017).
11. Omelkov, S., Nagirnyi, V., Vasil'ev, A. & Kirm, M. New features of hot intraband luminescence for fast timing. *J. Lumin.* **176**, 309–317 (2016).
12. R. M. Turtos, S. Gundacker, E. Auffray & P. Lecoq. Towards a metamaterial approach for fast timing in PET: experimental proof-of-concept. *Phys. Med. Biol.* **64**, 185018 (2019).
13. Turtos, R. M. et al. Ultrafast emission from colloidal nanocrystals under pulsed x-ray excitation. *J. Instrum.* **11**, P10015 (2016).
14. Achtstein, A. W. et al. Electronic structure and exciton-phonon interaction in two-dimensional colloidal CdSe nanosheets. *Nano Lett.* **12**, 3151–3157 (2012).
15. Ithurria, S., Tessier, M. D., Mahler, B., Lobo, R. P. S. M. & Efros, B. D. A. L. Colloidal nanoplatelets with two-dimensional electronic structure. *Nat. Mater.* **10**, 936 (2011).
16. Naeem, A. et al. Giant exciton oscillator strength and radiatively limited dephasing in two-dimensional platelets. *Phys. Rev. B* **91**, 121302 (2015).
17. Grim, J. Q. et al. Continuous-wave biexciton lasing at room temperature using solution-processed quantum wells. *Nat. Nanotechnol.* **9**, 891–895 (2014).
18. Woggon, U. et al. Huge binding energy of localized biexcitons in CdS/ZnS quantum structures. *Phys. Rev. B* **61**, 12632–12635 (2000).
19. Lecoq, P. Development of new scintillators for medical applications. *Nucl. Instrum. Methods Phys. Res. Sect. A, Accel. Spectrom. Detect. Assoc. Equip.* **809**, 130–139 (2016).
20. Bulin, A.-L. et al. Modelling energy deposition in nanoscintillators to predict the efficiency of the x-ray-induced photodynamic effect. *Nanoscale* **7**, 5744–5751 (2015).
21. Padilha, L. A., Bae, W. K., Klimov, V. I., Pietryga, J. M. & Schaller, R. D. Response of semiconductor nanocrystals to extremely energetic excitation. *Nano Lett.* **13**, 925–932 (2013).
22. Burešová, H. et al. Preparation and luminescence properties of ZnO:Ga-poly-styrene composite scintillator. *Opt. Express* **24**, 15289–15298 (2016).
23. Liu, C. et al. Facile single-precursor synthesis and surface modification of hafnium oxide nanoparticles for nanocomposite gamma-ray scintillators. *Adv. Funct. Mater.* **25**, 4607–4616 (2015).
24. Létant, S. E. & Wang, T.-F. Semiconductor quantum dot scintillation under gamma ray irradiation. *Nano Lett.* **6**, 2877–2880 (2006).
25. Létant, S. E. & Wang, T.-F. Study of porous glass doped with quantum dots or laser dyes under alpha irradiation. *Appl. Phys. Lett.* **88**, 103110 (2006).
26. Turtos, R. M. et al. Timing performance of ZnO:Ga nanopowder composite scintillators. *Physica. Status Solidi (RRL)* **10**, 843–847 (2016).
27. Bertrand, G. H. V., Polovitsyn, A., Christodoulou, S., Khan, A. H. & Moreels, I. Shape control of zincblende CdSe nanoplatelets. *Chem. Commun.* **52**, 11 975–11 978 (2016).
28. Antanovich, A., Prudnikov, A., Matsukovich, A., Achtstein, A. & Artemyev, M. Self-assembly of CdSe nanoplatelets into stacks of controlled size induced by ligand exchange. *J. Phys. Chem. C* **120**, 5764–5775 (2016).
29. Donegá, C. D. M. Synthesis and properties of colloidal heteronanocrystals. *Chem. Soc. Rev.* **40**, 1512–1546 (2011).
30. Yadav, S., Singh, A., Thulasidharan, L. & Sapra, S. Surface decides the photoluminescence of colloidal CdSe nanoplatelets based core/shell heterostructures. *J. Phys. Chem. C* **122**, 820–829 (2018).
31. Liu, C. et al. Transparent ultra-high-loading quantum dot/polymer nanocomposite monolith for gamma scintillation. *ACS Nano* **11**, 6422–6430 (2017).
32. Rabouw, F. T. et al. Temporary charge carrier separation dominates the photoluminescence decay dynamics of colloidal CdSe nanoplatelets. *Nano Lett.* **16**, 2047–2053 (2016).
33. Turtos, R. M. et al. Measurement of LYSO intrinsic light yield using electron excitation. *IEEE Trans. Nucl. Sci.* **63**, 475–479 (2016).
34. Turtos, R. M., Gundacker, S., Omelkov, S., Auffray, E. & Lecoq, P. Light yield of scintillating nanocrystals under x-ray and electron excitation. *J. Lumin.* **215**, 116613 (2019).
35. Gundacker, S., Turtos, R., Auffray, E. & Lecoq, P. Precise rise and decay time measurements of inorganic scintillators by means of x-ray and 511 keV excitation. *Nucl. Instrum. Methods Phys. Res. Sect. A, Accel. Spectrom. Detect. Assoc. Equip.* **891**, 42–52 (2018).
36. Piemonte, C. et al. Performance of NUV-HD silicon photomultiplier technology. *IEEE Trans. Electron Devices* **63**, 1111–1116 (2016).
37. Omelkov, S. I. et al. Scintillation yield of hot intraband luminescence. *J. Lumin.* **198**, 260–271 (2018).
38. Wanarak, C., Chewpraditkul, W. & Phunpueok, A. Light yield non-proportionality and energy resolution of Lu_{1.95}Y_{0.05}SiO₅:Ce and Lu₂SiO₅:Ce scintillation crystals. *Procedia Eng.* **32**, 765–771 (2012).
39. Rowland, C. E. et al. Picosecond energy transfer and multiexciton transfer outpaces Auger recombination in binary CdSe nanoplatelet solids. *Nat. Mater.* **14**, 484–489 (2015).
40. Agostinelli, S. et al. Geant4—a simulation toolkit. *Nucl. Instrum. Methods Phys. Res., Sect. A, Accel. Spectrom. Detect. Assoc. Equip.* **506**, 250–303 (2003).
41. Allison, J. et al. Geant4 developments and applications. *IEEE Trans. Nucl. Sci.* **53**, 270–278 (2006).
42. Tessier, M. D. et al. Efficient exciton concentrators built from colloidal core/crown CdSe/CdS semiconductor nanoplatelets. *Nano Lett.* **14**, 207–213 (2014).
43. Cates, J. W., Gundacker, S., Auffray, E., Lecoq, P. & Levin, C. S. Improved single photon time resolution for analog SiPMs with front end readout that reduces influence of electronic noise. *Phys. Med. Biol.* **63**, 185022 (2018).
44. Enquist, H. et al. FemtoMAX – an x-ray beamline for structural dynamics at the short-pulse facility of MAX IV. *J. Synchrotron Radiat.* **25**, 570–579 (2018).
45. Poikela, T. et al. Timepix3: a 65 K channel hybrid pixel readout chip with simultaneous ToA/ToT and sparse readout. *J. Instrum.* **9**, C05013–C05013 (2014).

ACKNOWLEDGEMENTS

This work was supported by the ERC Advanced Grant no. 338953 (TICAL), the ERC Starting Grant no. 714876 (PHOCONA), and Estonian Research Council (projects PUT1081, IUT2-26). A partial financial support from the Estonian Centre of Excellence TK141 by the EU through the European Regional Development Fund (TK141, project no. 2014-2020.4.01.15-0011) is gratefully acknowledged. The research have been developed in the frame of the Crystal Clear Collaboration and the Cost Action FAST TD1401. The authors are grateful to MAX-IV laboratory (Lund, Sweden) and FemtoMAX team lead by J. Larsson for the opportunity of scintillation decay experiment at 100-fs X-ray excitation. We are also most thankful for the collaboration maintained with the Medipix group at CERN, specially for the help of Lukas Tlustos and Jerome Alozy regarding technical support and the energy calibration of the Timepix detector.

AUTHOR CONTRIBUTIONS

R.M.T., S.G., I.M., E.A. and P.L., as a team, conceived the idea of implementing CdSe nanoplatelets in combination with standard scintillators for ultrafast timing applications. R.M.T. performed the characterization and drop-casting of the CdSe/CdS films on LYSO, the assembly of the CdSe-LYSO sampling pixel, the light yield measurements of CdSe-based nanocomposite and data analysis for most of the results. R.M.T. wrote the manuscript with contributions from all authors. S.G. designed the readout and performed the first CTR and rise time measurements of CdSe + LYSO pixel with 511 keV gammas. S.O. installed the TCSPC setup allowing for light yield measurements with X-rays and performed all cathodoluminescence experiments. As well, S.O., J.S., and M.K. performed the kinematic measurements at FemtoMAX. B.M. synthesized the CdSe/CdS used in the study and proceed with the solution treatment to obtain dry drop-casted films and the embedding procedure in PS. A.K. know-how was critical in the preparation of the CdSe in PS sample. C.D. and Z.M. characterized highly diluted CdSe/CdS films under different laser powers and X-ray excitation. A.V. produced and wrote all the theoretical considerations presented here.

COMPETING INTERESTS

The authors declare no competing interests.

ADDITIONAL INFORMATION

Supplementary information is available for this paper at <https://doi.org/10.1038/s41699-019-0120-8>.

Correspondence and requests for materials should be addressed to R.M.T.

Reprints and permission information is available at <http://www.nature.com/reprints>

Publisher's note Springer Nature remains neutral with regard to jurisdictional claims in published maps and institutional affiliations.



Open Access This article is licensed under a Creative Commons Attribution 4.0 International License, which permits use, sharing, adaptation, distribution and reproduction in any medium or format, as long as you give

appropriate credit to the original author(s) and the source, provide a link to the Creative Commons license, and indicate if changes were made. The images or other third party material in this article are included in the article's Creative Commons license, unless indicated otherwise in a credit line to the material. If material is not included in the article's Creative Commons license and your intended use is not permitted by statutory regulation or exceeds the permitted use, you will need to obtain permission directly from the copyright holder. To view a copy of this license, visit <http://creativecommons.org/licenses/by/4.0/>.

© The Author(s) 2019